Supplemental Materials

Molecular Biology of the Cell

Kama et al.

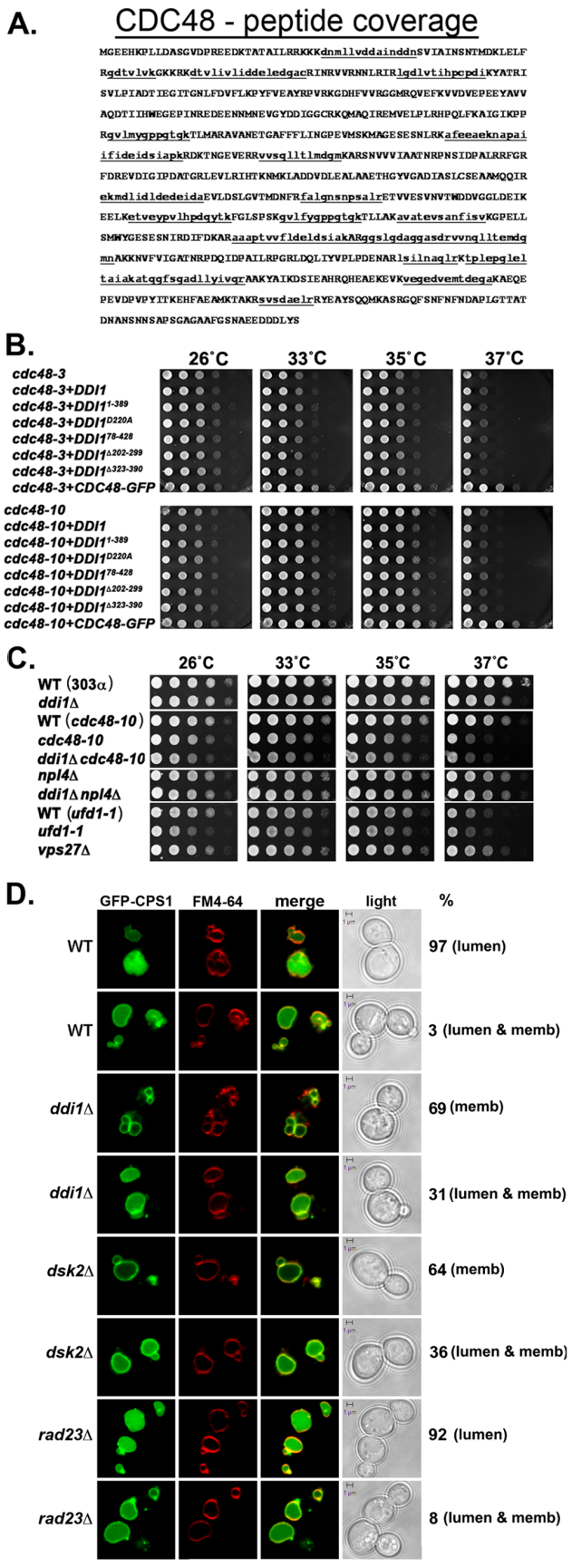

Figure S1. Ddi1 interacts physically with Cdc48. (A) Cdc48 coverage. The primary sequence of *S. cerevisiae* Cdc48 protein is presented. Underlined and lowercase amino acid designations

indicate peptide sequences identified by mass spectrometry in bands excised from SDS-PAGE-resolved and Coomassie-labeled HA-Ddi1 and HA-Ddi1^{D220A} precipitates. (**B). Over-expression of Ddi1 or Ddi1 truncation mutants do not ameliorate the growth defects of the *cdc48-3* or *cdc48-10* alleles.** *cdc48-3* and *cdc48-10* cells were transformed with vector alone (pAD54) or pAD54-based plasmids expressing HA-tagged Ddi1 or Ddi1 truncation mutants (*e.g.* Ddi1$^{1-389}$, Ddi1^{D220A}, Ddi1$^{78-428}$, Ddi1$^{\Delta 202-299}$, and Ddi1$^{\Delta 323-390}$) or a single-copy plasmid expressing Cdc48-GFP. Cells were grown to mid-log phase on glucose-containing medium at 26^{o}C before serial dilution (10-fold each) and plating by drops onto pre-warmed solid medium. Plates were grown for 2 to 3 days at the indicated temperatures before photo-documentation. (**C) The deletion of *DDI1* has no effect upon the growth of *cdc48* and *npl4* mutants.** WT control cells (*e.g.* W303 and the background strains for the *cdc48-10* and *ufd1-1* mutations), *ddi1*Δ, *cdc48-10, ddi1*Δ *cdc48-10, npl4*Δ, *ddi1*Δ *npl4*Δ, *ufd1-1*, and *vps27*Δ cells were grown to mid-log phase on glucose-containing medium at 26^{o}C before serial dilution (10-fold each) and plating by drops onto pre-warmed solid medium. Plates were grown for 2-3 days at the indicated temperatures before photo-documentation. **(D) Cps1 trafficking to the vacuole lumen is inhibited in cells lacking *DDI1* or *DSK2*, but not *RAD23*.** WT (W303 background) control cells and cells lacking *DDI1, DSK2*, or *RAD23* (*i.e. ddi1Δ*; *dsk2Δ rad23Δ* cells; W303 background) were transformed with a plasmid expressing GFP-Cps1. Cells were grown to mid-log at 26^{o}C, pulse-chase labeled with FM4-64, and examined by confocal microscopy. *Merge* indicates merger of the GFP and FM4-64 windows. *Light* indicates the DIC window. *%* indicates the percentage of cells having GFP-Cps1 localized to the vacuolar limiting membrane (memb), vacuolar lumen (lumen), or both (lumen & memb). Statistics are presented in Table 1. Size bar = 1μm.

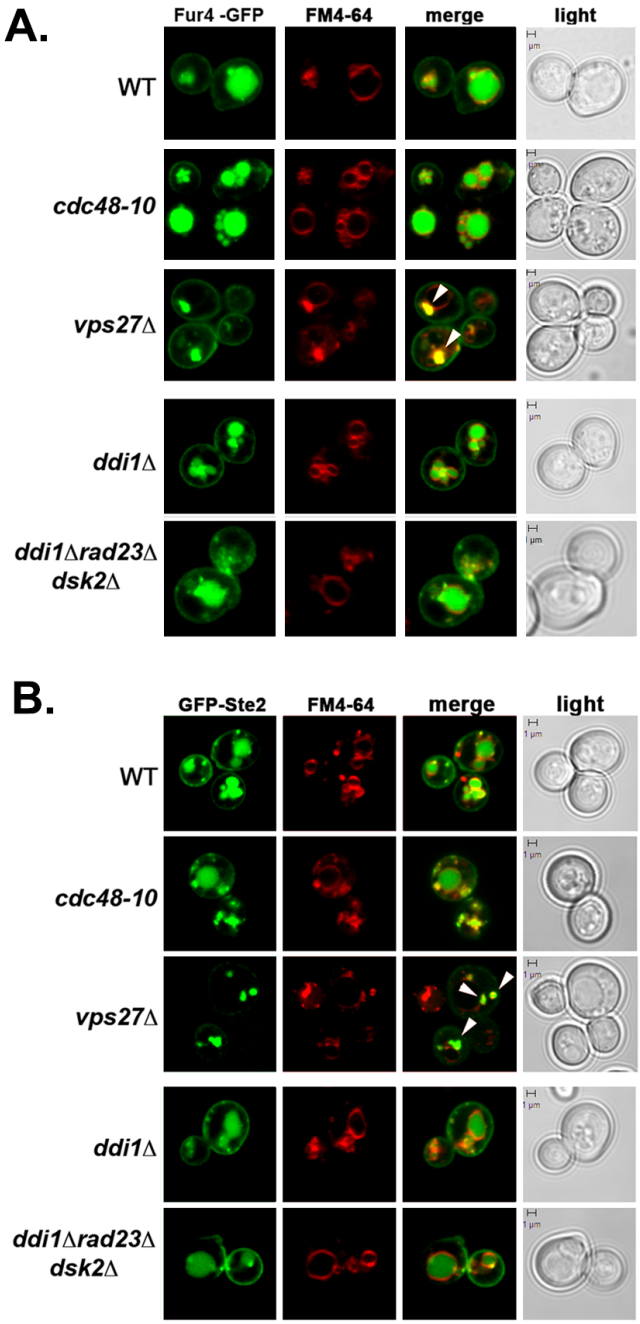

Figure S2. Trafficking of Fur4 and Ste2 to the vacuole is unaffected in cells bearing mutations in *CDC48* or the yeast ubiquilins. (A) Localization of Fur4-GFP to the plasma membrane and vacuole is not affected in cells bearing the *cdc48-10* allele or in *ddi1*Δ cells and cells lacking all three ubiquilins. WT control (W303) and *cdc48-10*, *vps27Δ, ddi1Δ*, and *ddi1*Δ *rad23*Δ *dsk2*Δ cells were transformed with a single-copy plasmid expressing Fur4-GFP. Cells were grown to mid-log phase on glucose-containing medium at 26°C at, pulse-chase labeled with FM4-64, and examined by confocal microscopy. White arrows indicate the position of the class E compartment wherein GFP-Fur4 and FM4-64 accumulate in *vps27Δ* cells (a class E *vps* mutant). *Merge* indicates merger of the GFP and FM4-64 windows. *Light* indicates the DIC window. Size bar = 1μm. Additional WT control cells of the *cdc48-10*, *vps27Δ*, and *ddi1Δ* backgrounds (*e.g.* KFY100 and BY4741, respectively) were examined, but gave identical results to that shown for the WT cells in the figure (data not shown). **(B) The intracellular localization of Ste2-GFP was not affected in *cdc48-10* cells or in cells either lacking *DDI1* or all three ubiquilins.** WT control (W303) and *cdc48-10*, *vps27Δ, ddi1Δ*, and *ddi1*Δ *rad23*Δ *dsk2*Δ cells

were transformed with a single-copy plasmid expressing Ste2-GFP. Cells were grown to mid-log phase on glucose-containing medium at 26^{o}C at, pulse-chase labeled with FM4-64, and examined by confocal microscopy. White arrows indicate the position of the class E compartment wherein Ste2-GFP and FM4-64 accumulate in *vps27Δ* cells (a class E *vps* mutant). *Merge* indicates merger of the GFP and FM4-64 windows. *Light* indicates the DIC window. Size bar = 1μm. Additional WT control cells of the *cdc48-10*, *vps27Δ*, and *ddi1Δ* backgrounds (*e.g.* KFY100 and BY4741, respectively,) were examined, but gave identical results to that shown for the WT cells in the figure (data not shown).

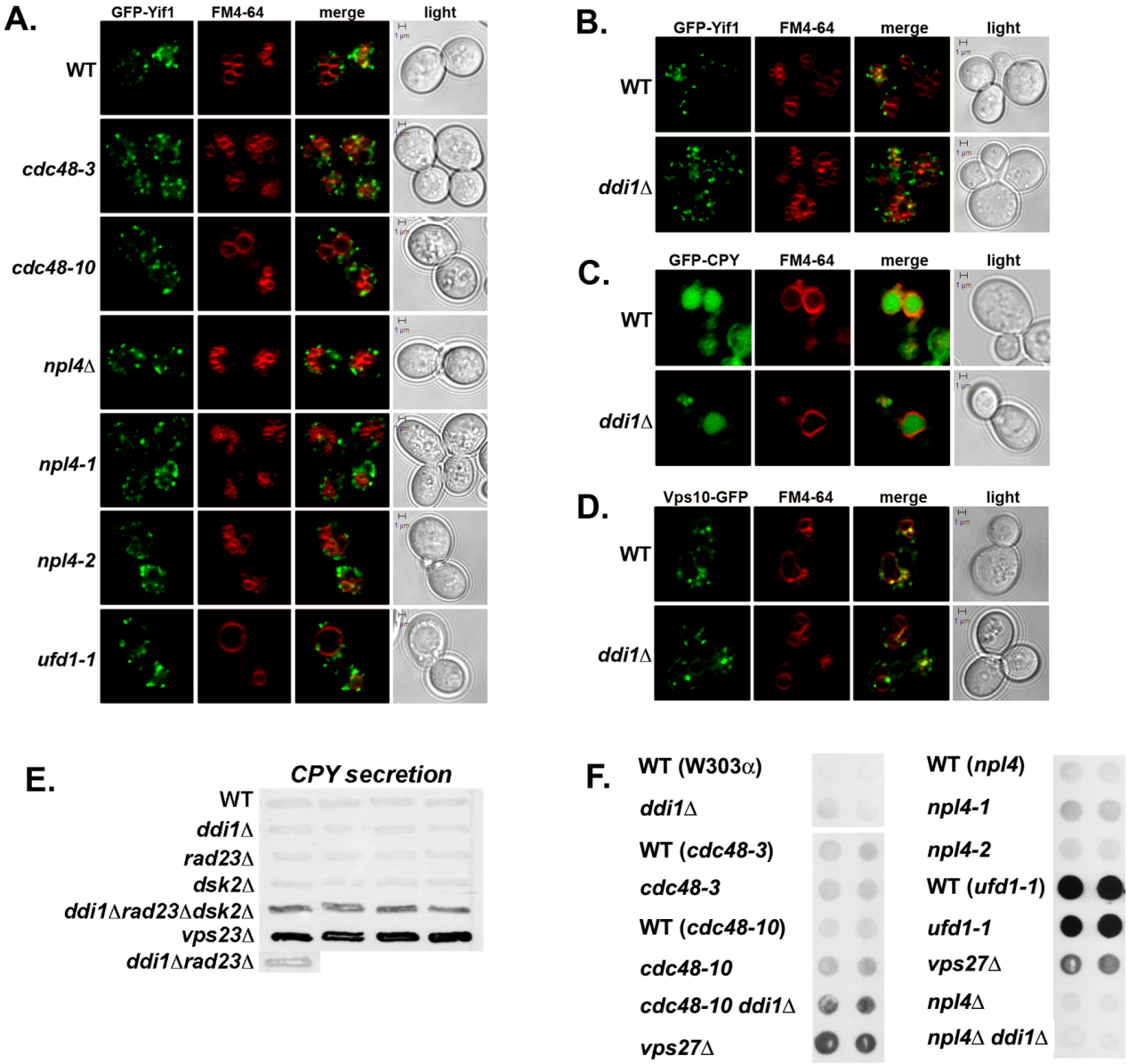

Figure S3. Individual mutations in *DDI1, DSK2, RAD23, CDC48, NPL4,* and *UFD1* do not affect CPY secretion, but combined *ddi1*Δ *dsk2*Δ *rad23*Δ and *ddi1*Δ *cdc48-10* mutations show a partial secretion effect. (A) Localization of GFP-Yif1 in WT, *cdc48-3, cdc48-10, npl4*Δ*, npl4-1, npl4-2,* and *ufd1-1* cells. WT control (*e.g.* BY4741 and W303 backgrounds and background strains for the *cdc48-3*, *cdc48-10* and *ufd1-1* mutations), *cdc48-3, cdc48-10, npl4*Δ*, npl4-1, npl4-2,* and *ufd1-1* cells were transformed with a single-copy plasmid expressing GFP-Yif1. Cells were grown to mid-log phase cells on glucose containing medium at 26°C, pulse-chase labeled with FM4-64, and examined by confocal microscopy. *Merge* indicates merger of the GFP and FM4-64 windows. *Light* indicates the DIC window. Size bar = 1μm. **(B) Localization of GFP-Yif1, GFP-CPY, and Vps10-GFP in WT and *ddi1Δ* cells.** WT control (W303), and *ddi1Δ* cells were transformed with a single-copy plasmid expressing GFP-Yif1, Cells were grown to mid-log phase on glucose-containing medium at 26°C, pulse-chase labeled with FM4-64, and examined by confocal microscopy. *Merge* indicates merger of the GFP and FM4-64 windows. *Light* indicates the DIC window. Size bar = 1μm. **(C) Localization of GFP-CPY in WT and *ddi1Δ* cells.** WT control (W303), and *ddi1Δ* cells were transformed with a

single-copy plasmid expressing CPY^{1-50}-GFP. Cells were grown to mid-log phase on glucose-containing medium at 26°C, shifted to galactose-containing medium for 12h at 26°C to induce expression, pulse-chase labeled with FM4-64, and examined by confocal microscopy. *Merge* indicates merger of the GFP and FM4-64 windows. *Light* indicates the DIC window. Size bar = 1μm. (**D) Localization of Vps10-GFP in wild-type and *ddi1Δ* cells.** WT control (W303), and *ddi1Δ* cells were transformed with a single-copy plasmid expressing Vps10-GFP. Cells were grown to mid-log phase cells on glucose containing medium at 26°C, pulse-chase labeled with FM4-64, and examined by confocal microscopy. *Merge* indicates merger of the GFP and FM4-64 windows. *Light* indicates the DIC window. Size bar = 1μm. (**E) Combined deletions in the ubiquilin paralogs leads to CPY secretion.** WT yeast (BY4741) and various deletion mutants (*e.g. ddi1Δ, rad23Δ, ddi1Δ rad23Δ, dsk2Δ, ddi1Δ rad23Δ dsk2Δ,* and *vps23Δ* cells) were patched out and grown on solid medium, replica plated onto nitrocellulose filters and subjected to anti-CPY immunoblot assay, as detailed in below in the detailed in the *Materials and Methods*. **(F) Combined *ddi1Δ* and *cdc48-10* mutations lead to a CPY secretion phenotype.** WT control (*e.g.* W303 and the backgrounds for the *cdc48-3*, *cdc48-10, npl4*, and *ufd1-1* cells), *ddi1Δ, cdc48-3*, *cdc48-10, cdc48-10 ddi1Δ, npl4-1, npl4-2, ufd1-1, npl4*Δ*, npl4*Δ *ddi1*Δ*,* and *vps27Δ* cells were grown on glucose-containing medium at 26°C before serial dilution (10-fold each) and plating by drops onto pre-warmed solid medium. Plates were grown for 2-3 days, replica plated onto nitrocellulose filters, and subjected to anti-CPY immunoblot assay, as detailed in the *Materials and Methods*.

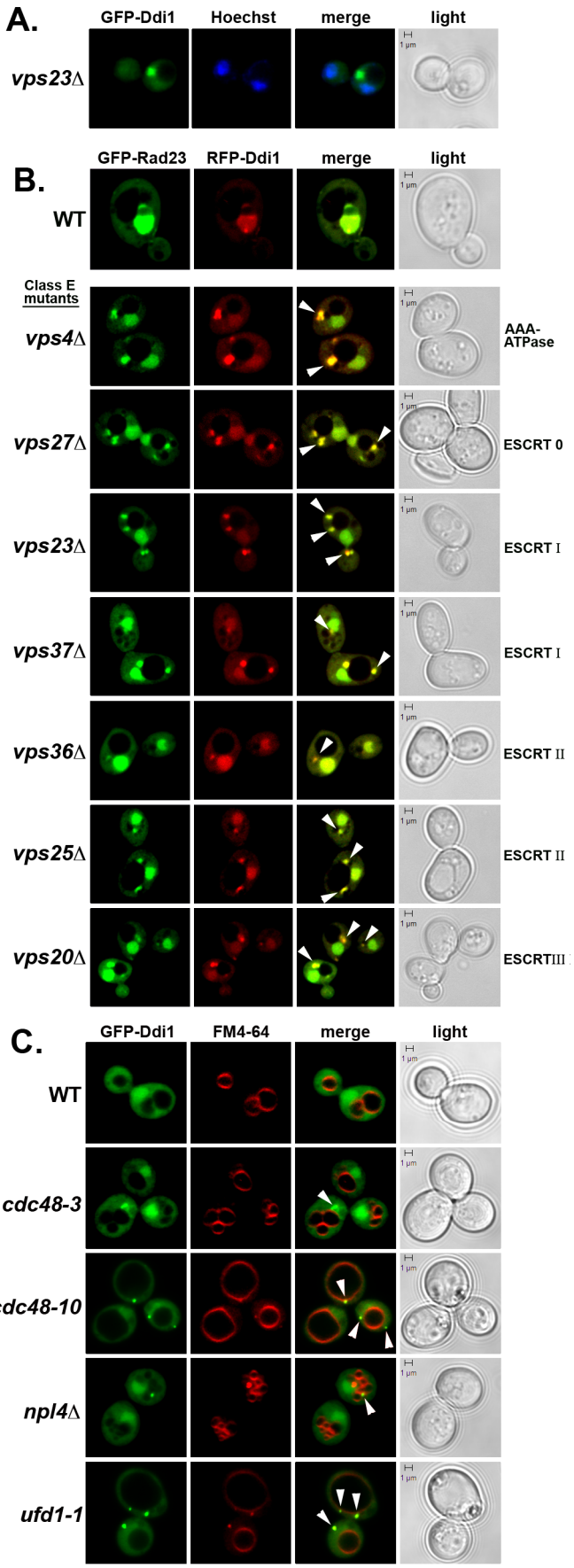

Figure S4. Ddi1 and Rad23 co-label the perivacuolar class E compartment in MVB mutants and Ddi1 labels a perivacuolar compartment in cells bearing mutations in *CDC48*, *NPL4*, and *UFD1*. (A) GFP-Ddi1-labeled puncta in *vps23*Δ cells are non-nuclear. *vps23*Δ cells carrying the genome-integrated copy of *GFP-DDI1* under the control of a *GAL* promoter

(GGY13 cells) were grown to mid-log phase on galactose-containing medium and labeled with Hoechst dye (2μg/ml) for 10min prior to visualization by confocal microscopy. *Merge* indicates merger of the GFP and Hoechst windows. *Light* indicates the DIC window. Size bar = 1μm. (**B) GFP-Rad23 and RFP-Ddi1 co-localize in wild-type cells and class E/MVB mutants**. Class E mutant cells (*e.g. vps4*Δ, *vps27*Δ*, vps23*Δ, *vps37*Δ, *vps36*Δ, *vps25*Δ, and *vps20*Δ cells) were transformed with a multi-copy plasmids expressing GFP-Rad23 and RFP-Ddi1. Cells were grown to mid-log phase cells on glucose-containing medium at 26^{o}C, pulse-chase labeled with FM4-64, and examined by confocal microscopy. *Merge* indicates merger of the GFP and RFP windows. *Light* indicates the DIC window. Size bar = 1μm. **(C) In addition to nuclear and cytoplasmic labeling, Ddi1 localizes to a perivacuolar compartment in cells bearing mutations in *CDC48, NPL4,* and *UFD1.*** WT control (*e.g.* BY4741 and the backgrounds for the *cdc48*-3, *cdc48-10*, and *ufd1-1* strains), *cdc48*-3, *cdc48-10*, *npl4*Δ, and *ufd1-1* cells were transformed with a multi-copy plasmid expressing GFP-Ddi1 Mid-log phase cells grown on glucose containing medium at 26^{o}C, pulse-chase labeled with FM4-64, and examined by confocal microscopy. *Merge* indicates merger of the GFP and FM4-64 windows. *Light* indicates the DIC window. Size bar = 1μm. Only the WT background for *cdc48-10* cells (KFY100) is shown; similar results were obtained with the other backgrounds (data not shown).

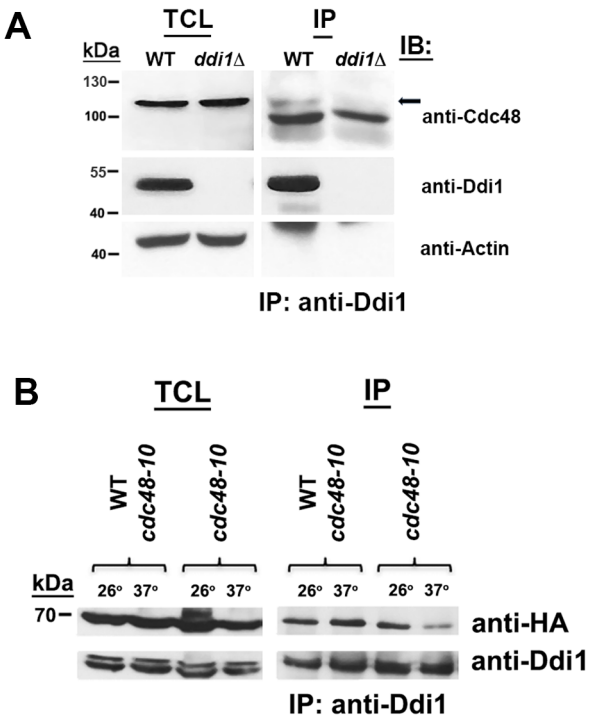

Figure S5. Endogenous Ddi1 binds endogenous Cdc48, while its binding to Npl4 is reduced upon the attenuation of Cdc48 function. A. Endogenous Ddi1 and Cdc48 co-precipitate. WT control and *ddi1Δ* cells were grown to mid-log phase on glucose-containing YPD medium at 26^{o}C and processed for immunoprecipitation using anti-Ddi1 antibodies, as described in the *Materials and Methods*. Native endogenously-expressed Cdc48 was detected using polyclonal anti-Cdc48 antibodies (1:500) and native endogenously-expressed Ddi1 was detected using polyclonal anti-Ddi1 antibodies (1:3000). **B. Ddi1 binding to Npl4 is reduced upon the attenuation of Cdc48 function.** WT control (*cdc48-10* background) and *cdc48-10* cells were transformed with a multi-copy plasmid expressing HA-Npl4. Cells were grown to mid-log phase cells on glucose-containing synthetic medium at 26^{o}C and either maintained at 26^{o}C or shifted to 37^{o}C for 1hr. Cells were processed for immunoprecipitation using anti-Ddi1 antibodies, as described in the *Materials and Methods*. Npl4 was detected using monoclonal anti-HA antibodies (1:1000) and native Ddi1 was detected using polyclonal anti-Ddi1 antibodies (1:3000). In this representative experiment, the level of Npl4 bound to Ddi1 declined by 56% in *cdc48-10* cells after the temperature shift, while it was unchanged (after normalization for precipitated Ddi1 levels) in the WT background.

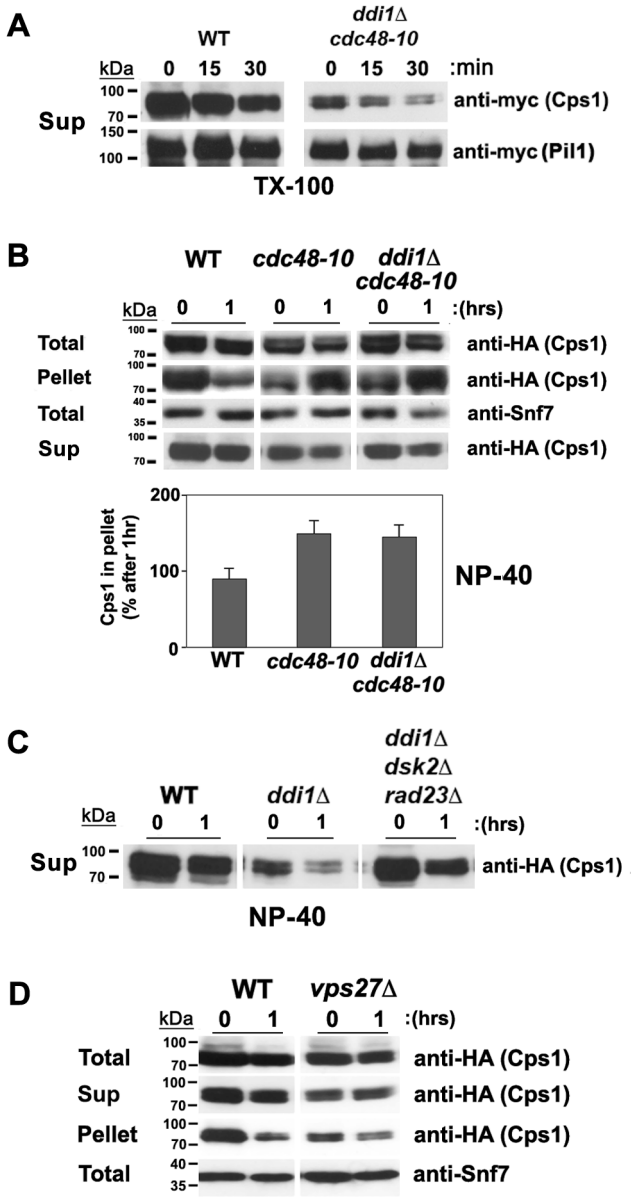

Figure S6. Soluble Cps1 declines while insoluble Cps1 increases in *cdc48-10, ddi1Δ, cdc48-10 ddi1Δ,* and *ddi1Δ dsk1Δ rad23Δ* cells. (A) The fraction of detergent-soluble myc-Cps1, but not myc-Pil1, decreases in *cdc48-10 ddi1Δ* cells after CHX treatment. Yeast expressing endogenous myc-Cps1 or myc-Pil1 from their genomic loci in WT and *cdc48-10 ddi1Δ* cells were subjected to a cycloheximide (CHX)-chase degradation/sedimentation assay to resolve the amount of TX-100 detergent-soluble Cps1 or Pil1 in the pellet fraction, as described under *Materials and Methods*. Samples of were removed after 0, 15, and 30min of CHX treatment before processing to determine the relative amounts of myc-Cps1 in the total, pellet, and supernatant (see Figure 5A and B for total and pellet) fractions using anti-myc antibodies. The amount of soluble and insoluble Cps1 after 1hr was normalized to the loading control, after which the percentage was calculated relative to the amount at 0hrs. A representative experiment is shown whereby myc-Cps1 levels in the detergent-soluble fraction (*i.e.* supernatant) decline substantially over time, whereas as myc-Pil1 levels remain relatively steady. kDa = kilodaltons **(B) The fraction of NP40-insoluble Cps1 increases in *cdc48-10* and *cdc48-10 ddi1Δ* cells.** WT control cells (*cdc48-10* background), *cdc48-10*, and *cdc48-10 ddi1Δ* cells transformed with a plasmid expressing HA-Cps1 were subjected to the cycloheximide-chase degradation/sedimentation assay shown in *A* to resolve the amount of NP-40 detergent-insoluble and -soluble Cps1, as described under *Materials and Methods*. Samples of the total cell lysate

(TCL; Total), insoluble pellet (Pellet), and soluble (*i.e.* supernatant; Sup) fraction were resolved by SDS-PAGE and detected in Westerns with anti-HA (1:1000) abs. TCL samples were also probed with anti-Snf7 abs (1:2000) as a loading control (Snf7 is not degraded upon CHX treatment, unlike actin). The amount of soluble and insoluble Cps1 after 1hr was normalized to the loading control, after which the percentage was calculated relative to the amount at 0hrs. A representative experiment is shown, whereby the level of insoluble Cps1 increased by 71% and 76% over that of WT cells in the *cdc48-10* and *cdc48-10 ddi1Δ* pellet fractions after 1hr, respectively. A histogram showing average±standard deviation of 4 experiments is shown beneath. **(C) The fraction of NP-40 detergent-soluble Cps1 decreases in *ddi1Δ* and *ddi1Δ dsk2Δ rad23Δ* cells.** WT control cells (W303), *ddi1Δ,* and *ddi1Δ dsk2Δ rad23Δ* cells expressing HA-Cps1 were subjected to the same procedure as in *A* and the percentage of soluble Cps1 in the supernatant fraction after 1hr was calculated after the normalization for gel loading and expression (see Figure 5C for results with total and pellet fractions). A representative experiment is shown. **(D) The detergent-insoluble Cps1 fraction decreases in *vps27Δ* cells.** WT control cells and *vps27Δ* cells transformed with a plasmid expressing HA-Cps1 were subjected to the cycloheximide-chase degradation/sedimentation assay described in *A* to resolve the amount of NP-40 detergent-insoluble and -soluble Cps1. Samples of the total cell lysate (TCL; Total), insoluble pellet (Pellet), and soluble (*i.e.* supernatant; Sup) fractions were resolved by SDS-PAGE and detected in Westerns with anti-HA (1:1000) abs. TCL samples were also probed with anti-Snf7 abs (1:2000) as a loading control. The amount of insoluble Cps1 in the pellet was calculated relative to the amount at 0hrs, as described above. A representative experiment is shown.

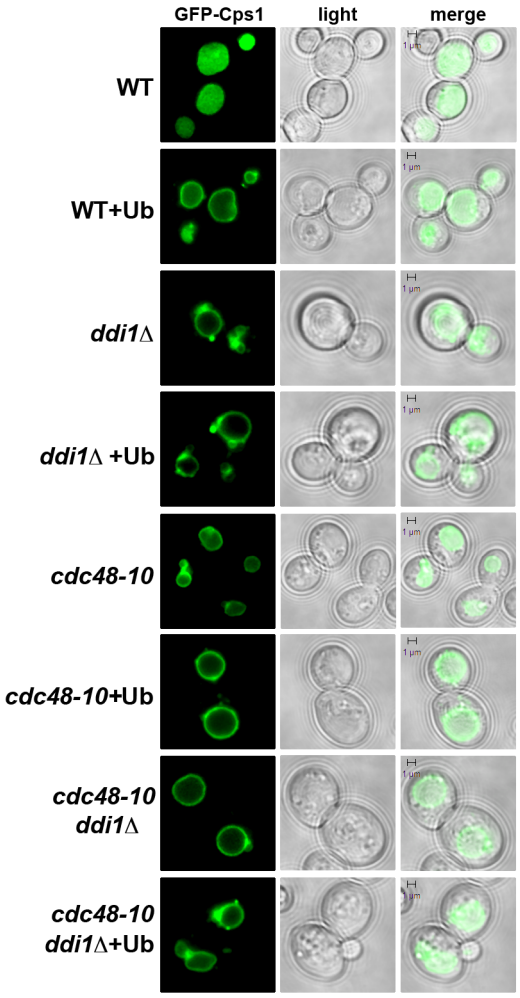

Figure S7. Ubiquitin over-expression does not rescue Cps1 mistrafficking in *ddi1Δ*, *cdc48-10*, and *cdc48-10 ddi1Δ* cells. WT control (*e.g.*W303 and the backgrounds for the *cdc48-10*, strains), *ddi1Δ*, *cdc48-10*, and *cdc48-10 ddi1Δ* cells were transformed with multicopy plasmids expressing GFP-Cps1 and ubiquitin (Ub; *UBL4*). Cells grown to mid-log phase on glucose containing medium at 26^{o}C were examined by confocal microscopy. *Merge* indicates merger of the GFP and light windows. *Light* indicates the DIC window. Size bar = 1μm. Only one WT cell background (*e.g.* W303) is shown, the others were identical with respect to Cps1 localization.

Table S1. Yeast strains used in this study

Name	Genotype	Source
W303-1b	*MAT*α *can1-100 his3-2,15 leu2-3,112 lys2-1 trp1-1 ura3-1 ade2-1*	J. Gerst
BY4741	*MAT*a *his3Δ1 leu2Δ0 met15Δ0 ura3Δ0*	Euroscarf
yPC1507 (*cdc48-3* WT background)	*MAT*a *ura3-52 his3Δ200 leu2Δ1 trp1Δ63*	P. Carvalho
yPC1614 (*cdc48-3*)	*MAT*a *ura3-52 his3Δ200 leu2Δ1 trp1Δ63 cdc48-3^{ts}*	P. Carvalho
RK8 (*cdc48-3 ddi1*Δ)	*MAT*a *ura3-52 his3Δ200 leu2Δ1 trp1Δ63 cdc48-3^{ts} ddi1Δ::NAT1*	This study
KFY100 (*cdc48-10* WT background)	*MAT*a *his4-619 leu2-3,112 ura3-52*	S. Bar-Nun
KFY194 (*cdc48-10*)	*MAT*a *his4-619 leu2-3,112 ura3-52 cdc48-10^{ts}*	S. Bar-Nun
SBN 100 (*cdc48-10* WT background)	*MAT*a *his4-619 leu2-3,112 ura3-52 trp1::LEU2*	S. Bar-Nun
SBN194 (*cdc48-10*)	*MAT*a *his4-619 leu2-3,112 ura3-52 cdc48-10^{ts} trp1::LEU2*	S. Bar-Nun
RK10 (*cdc48-10 ddi1*Δ)	*MAT*a *his4-619 leu2-3,112 ura3-52 cdc48-10^{ts} ddi1Δ::NAT1*	This study
cps1Δ	*MAT*a *his3Δ1 leu2Δ met15Δ0 ura3Δ0 cps1Δ::kanMX*	Euroscarf
VL2 (*ddi1Δ*; W303-1a background)	*MAT*a *his3-11,15 leu2-3,112 trp1-1 ade2-1 ddi1Δ::URA3*	J. Gerst
*ddi1*Δ (W303-1b background)	*MAT*α *can1-100 his3-11,15 leu2-3,112 lys2-1 trp1-1 ura3-1 ade2-1 ddi1Δ::NAT1*	This study
ddi1Δ (BY4741 background)	*MAT*a *his3Δ1 leu2Δ met15Δ0 ura3Δ0 ddi1Δ::kanMX*	Euroscarf
GGY21 (*ddi1Δ rad23Δ*)	*MAT*a *his3Δ1 leu2Δ met15Δ0 ura3Δ0 rad23Δ::kanMX ddi1Δ::URA3*	This study
GGY22 (*ddi1*Δ *rad23*Δ *dsk2*Δ)	*MAT*a *leuΔ0 met15Δ0 rad23Δ::HIS3 ddi1Δ::URA3 dsk2Δ::kanMX*	This study
GGY10 (*ddi1*Δ *vps23*Δ)	*MAT*a *his3Δ1 leu2Δ met15Δ0 ura3Δ0 vps23Δ::kanMX ddi1Δ::URA3*	This study
GGY13 (*GAL-GFP-DDI1 vps23Δ*)	*MAT*a *leuΔ0 met15Δ0 ura3Δ0 GAL1-GFP-DDI1::HIS3 vps23Δ::kanMX*	This study
doa1Δ	*MAT*a *his3Δ1 leu2Δ met15Δ0 ura3Δ0 doa1Δ::kanMX*	Euroscarf
RK11 *dsk2*Δ (W303-1b background)	*MAT*α *can1-100 his3-11,15 leu2-3,112 lys2-1 trp1-1 ura3-1 ade2-1 dsk2Δ::NAT1*	This study
YYH46 (*NPL4*)	*MAT*a *ura3-52 leu2Δ1 trp1Δ63* (originally PSY580)	P. Carvalho
YYH1 (*npl4-1*)	*MAT*a *ura3-52 leu2Δ1 trp1Δ63 npl4-1^{ts}* (originally PSY2340)	P. Carvalho
YYH2 (*npl4-2*)	*MAT*a *ura3-52 leu2D1 trp1Δ63 npl4-2^{ts}* (originally PSY2341)	P. Carvalho
npl4Δ	*MAT*a *his3Δ1 leu2Δ met15Δ0 ura3Δ0 npl4Δ::kanMX*	Euroscarf
RK9 (*npl4Δ ddi1Δ*)	*MAT*a *his3Δ1 leu2Δ met15Δ0 ura3Δ0 npl4Δ::kanMX ddi1Δ::NAT1*	This study
JBY120 (*SNF7-RFP*)	*MAT his3Δ1 leu2Δ0 lys2Δ0 ura3Δ0 SNF7-RFP:: KanMX4*	W. Huh
RK12 *rad23Δ* (W303-1b background)	*MAT*α *can1-100 his3-11,15 leu2-3,112 lys2-1 trp1-1 ura3-1 ade2-1 rad23Δ::NAT1*	This study
TCY6210 WT	*MAT*α *leu2-3, 112 ura3-52 his3-Δ200 trp1-Δ901 lys2-801 suc2Δ9*	S. Emr
SSY22 (*rsp5^{ts}*)	*MAT*a *leu2-3, 112 ura3-52 his3-Δ200 trp1-Δ901 ade2-101 suc2-Δ9 rsp5-326*	S. Emr
YYH3 (*UFD1*)	*MAT*a *his4-519 ura3-52 ade1-100 leu2-3,112* (originally BWG1-7a)	P. Carvalho
YYH4 (*ufd1-1*)	*MAT*a *ufd1-1* (derivative of BWG1-7a; originally PM373)	P. Carvalho
*vps4*Δ	*MAT*a *his3Δ1 leu2Δ met15Δ0 ura3Δ0 vps23Δ::kanMX*	Euroscarf
*vps23*Δ	*MAT*a *his3Δ1 leu2Δ met15Δ0 ura3Δ0 vps4Δ::kanMX*	Euroscarf
vps27Δ	*MAT*a *his3Δ1 leu2Δ met15Δ0 ura3Δ0 vps27Δ::kanMX*	Euroscarf
vps37Δ	*MAT*a *his3Δ1 leu2Δ met15Δ0 ura3Δ0 vps37Δ::kanMX*	Euroscarf

RK12 [myc(x9)-Cps1]	*MAT*α *can1-100 his3-2,15 leu2-3,112 lys2-1 trp1-1 ura3-1 ade2-1 CPS1::myc(x9)-CPS1*	This study
RK13 [*cdc48-10 ddi1*Δ myc(x9)-Cps1]	*MAT*a *his4-519 leu2-3,112 ura3-52 cdc48-10^{ts} ddi1*Δ*::NAT1 CPS1::myc(x9)-CPS1*	This Study
RK14 [*cdc48-10 ddi1*Δ myc(x9)-Pil]	*MAT*a *his4-519 leu2-3,112 ura3-52 cdc48-10^{ts} ddi1*Δ*::NAT1 PIL1::myc(x9)-PIL1*	This Study

Table S2. Plasmids used in this study

Plasmid name	Gene expressed	Vector	Sites of cloning	Copy number	Selectable marker	Source
pAD54	*HA*			*2μ*	*LEU2*	J. Gerst
pADH-HA-GFP	*HA-GFP*	pAD54	*Sal*I/*Sac*I	*2μ*	*LEU2*	J. Gerst
pADH-HA-DDI1	*HA-DDI1*	pAD54	*Sal*I/*Sac*I	*2μ*	*LEU2*	J. Gerst
pADH-DDI1$^{1-163}$	*HA-DDI1$^{1-163}$*	pAD54	*Sal*I/*Sac*I	*2μ*	*LEU2*	J. Gerst
pADH-DDI1$^{1-326}$	*HA-DDI1$^{1-326}$*	pAD54	*Sal*I/*Sac*I	*2μ*	*LEU2*	J. Gerst
pADH-DDI1$^{1-389}$	*HA-DDI1$^{1-389}$*	pAD54	*Sal*I/*Sac*I	*2μ*	*LEU2*	J. Gerst
pADH-DDI1^{D220A}	*HA-DDI1^{D220A}*	pAD54	*Sal*I/*Sac*I	*2μ*	*LEU2*	J. Gerst
pADH-DDI1$^{78-428}$	*HA-DDI1$^{78-428}$*	pAD54	*Sal*I/*Sac*I	*2μ*	*LEU2*	J. Gerst
pADH- DDI1$^{\Delta 202-299}$	*HA-DDI1$^{\Delta 202-298}$*	pAD54	*Sal*I/*Sac*I	*2μ*	*LEU2*	J. Gerst
pADH- DDI1$^{\Delta 323-344}$	*HA-DDI1$^{323-344}$*	pAD54	*Sal*I/*Sac*I	*2μ*	*LEU2*	J. Gerst
pADH-DDI1$^{78-326}$	*HA-DDI1$^{78-326}$*	pAD54	*Sal*I/*Sac*I	*2μ*	*LEU2*	J. Gerst
pADH- DDI1$^{\Delta 323-390}$	*HA-DDI1$^{\Delta 323-390}$*	pAD54	*Sal*I/*Sac*I	*2μ*	*LEU2*	J. Gerst
pADH-GFP- DDI1	*HA-GFP-DDI1*	pAD54	*Sal*I/*Sac*I	*2μ*	*LEU2*	J. Gerst
pADH- GFP-DDI1$^{1-75}$	*HA-GFP-DDI1$^{1-75}$*	pAD54	*Sal*I/*Sac*I	*2μ*	*LEU2*	J. Gerst
pADH-GFP-DDI1$^{1-163}$	*HA-GFP-DDI1$^{1-163}$*	pAD54	*Sal*I/*Sac*I	*2μ*	*LEU2*	J. Gerst
pADH-GFP-DDI1$^{1-326}$	*HA-GFP-DDI1$^{1-326}$*	pAD54	*Sal*I/*Sac*I	*2μ*	*LEU2*	J. Gerst
pADH-GFP-DDI1$^{1-389}$	*HA-GFP-DDI1$^{1-389}$*	pAD54	*Sal*I/*Sac*I	*2μ*	*LEU2*	J. Gerst
pADH-GFP-DDI1^{D220A}	*HA-GFP-DDI1^{D220A}*	pAD54	*Sal*I/*Sac*I	*2μ*	*LEU2*	J. Gerst
pADH-GFP-DDI1$^{78-428}$	*HA-GFP-DDI1$^{78-428}$*	pAD54	*Sal*I/*Sac*I	*2μ*	*LEU2*	J. Gerst
pADH-GFP-DDI1$^{\Delta 202-299}$	*HA-GFP-DDI1$^{\Delta 202-298}$*	pAD54	*Sal*I/*Sac*I	*2μ*	*LEU2*	J. Gerst
pADH-GFP-DDI1$^{\Delta 323-344}$	*HA-GFP-DDI1$^{\Delta 323-344}$*	pAD54	*Sal*I/*Sac*I	*2μ*	*LEU2*	J. Gerst
pADH-GFP-DDI1$^{78-326}$	*HA-GFP-DDI1$^{78-326}$*	pAD54	*Sal*I/*Sac*I	*2μ*	*LEU2*	J. Gerst
pADH-RFP-DDI1	*HA-RFP-DDI1*	pAD54	*Sal*I/*Sac*I	*2μ*	*LEU2*	This study
pADH-GFP-RAD23	*HA-GFP-RAD23*	pAD54	*Sal*I/*Sac*I	*2μ*	*LEU2*	This study
pGOGFP-CPS1	*GFP-CPS1*	pRS426	-	*2μ*	*URA3*	C. Stefan
pMB118	*GFP-CPS1*		-	*2μ*	*LEU2*	M. Babst
pADH-CPS1	*HA-CPS1*	pAD54	*Sma*I-*Sac*I	*2μ*	*LEU2*	This study
pGO-GFP-VPS27	*GFP-VPS27*	pRS426	*Bam*HI	*2μ*	*URA3*	S. Emr
pADH-RFP-VPS27	*HA-RFP-VPS27*	pAD54	*Sal*I/*Sac*I	*2μ*	*LEU2*	J. Gerst
pRS315-STE2-GFP	*STE2-GFP*	pRS315	-	*CEN*	*LEU2*	R. Piper
pUG45-CDC48-GFP	*CDC48-GFP*	pUG45		*CEN*	*URA3*	This study
pADH-GFP-SNX4	*HA-GFP-SNX4*	pAD54	*Sal*I	*2μ*	*LEU2*	J. Gerst
pRS313-VPS10-GFP	*HA-VPS10-RFP*	pRS313	*Bam*HI	*CEN*	*HIS3*	J. Gerst
pRS313-VPS10-RFP	*HA-VPS10-RFP*	pRS313	*Bam*HI	*CEN*	*HIS3*	This study
pAD54-GFP-NPL4	*HA-GFP-NPL4*	pAD54	*Sma*I-*Sac*I	*2μ*	*LEU2*	This study
pRS316-FUR4-GFP	*HA-FUR4-GFP*	pAD54	*Bam*HI	*CEN*	*LEU2*	This Study
pRS316-GFP-YIF1	*HA-GFP-YIF1*	pRS316	*Bam*HI	*CEN*	*URA3*	J. Gerst
pGALΔBglII-CPY(1-50)-GFP	*CPY$^{1-50}$-GFP*	pGALΔ BglII		*CEN*	*URA3*	D. Deloche
pRS425-UBL4	*UBL4*	pRS425		*2μ*	*HIS3*	M. Babst